# Novel insights in thrombosis pathophysiology using Mice with Impaired anticoagulation

Heestermans, M.

7

# Predilection of Low Protein C-induced Spontaneous Atherothrombosis for the Right Coronary Sinus in Apolipoprotein E deficient mice

Marco Heestermans*
Amber B Ouweneel*
Jasmin Hassan
Meander Kloosterman
Marion JJ Gijbels
Pieter H Reitsma
Bart JM van Vlijmen**
Miranda Van Eck**

***: These authors contributed equally*

*Manuscript submitted for publication*

## ABSTRACT

Silencing of anticoagulant protein C using RNA interference (si*Proc*) evokes low incident but spontaneous atherothrombosis in the aortic root of apolipoprotein E–deficient (*Apoe*$^{-/-}$) mice. The aims of the current study were 1) to analyze if plaque characteristics or circulating factors could be linked to atherothrombosis susceptibility, 2) to increase the incidence of atherothrombosis by transiently increasing blood pressure, and 3) to direct atherothrombosis to an additional predefined vascular site by applying a semi-constrictive collar around the carotid artery.

In the current study, si*Proc*-driven spontaneous atherothrombosis in the aortic root of *Apoe*$^{-/-}$ mice was reproduced and occurred at an incidence of 23% (9 out of 39 mice), while the incidence of collar-induced atherothrombosis in the carotid artery was 2.6% (1 out of 39 mice). Treatment with phenylephrine, to transiently increase blood pressure, did not increase atherothrombosis in the aortic root of the *Apoe*$^{-/-}$ mice nor in the carotid arteries with collars. Plaques in the aortic root with an associated thrombus were lower in collagen and macrophage content, and mice with atherothrombosis had significantly more circulating platelets. Plasma protein C, white blood cell counts, total cholesterol, fibrinogen, and serum amyloid A were not different amongst si*Proc* treated mice with or without thrombosis. Remarkably, our data revealed that thrombus formation preferably occurred on plaques in the right coronary sinus of the aortic root.

In conclusion, there is a predilection of low protein C-induced spontaneous atherothrombosis in *Apoe*$^{-/-}$ mice for the right coronary sinus, a process that is associated with an increase in platelets and plaques lower in collagen and macrophage content.






## INTRODUCTION

Atherothrombosis, characterized by superimposed thrombus formation overlying a ruptured or eroded atherosclerotic lesion, is the cause of death for more than 14 million individuals per year worldwide (in 2015, World Health organization, www.who.int). Atherogenesis, which can eventually lead to atherothrombosis, has been studied extensively in genetically modified mouse models: When mice deficient for genes involved in cholesterol metabolism, such as apolipoprotein E knockout (*Apoe*$^{-/-}$) mice or low-density lipoprotein receptor knockout (*Ldlr*$^{-/-}$) mice, are fed a cholesterol-rich diet, they rapidly develop atherosclerotic plaques (1-3). These mouse models have proven to be valuable for unravelling the pathophysiology of atherosclerosis (4, 5). However, unlike in humans, atherothrombosis does not occur spontaneously in mice, although some signs of rupture or erosion and intraplaque hemorrhage have been recorded (6-8).

Recently, we showed that transient (7 days) siRNA mediated lowering of the natural anticoagulant protein C (si*Proc*) in atherosclerotic *Apoe*$^{-/-}$ mice induced superimposed thrombus formation on atherosclerotic plaques in the aortic root (9). Although the incidence of this unique phenotype was low (1 out of 4 and 3 out of 25 in two independent experiments, cumulative incidence of 14%), our novel mouse model might be of use to better understand the pathophysiology of atherothrombosis. Moreover, a mouse model of atherothrombosis will be instrumental for the development of novel strategies for the treatment and prevention of atherothrombosis in humans.

Currently, however, the factors which determine when and where a thrombus develops on top of an atherosclerotic plaque are still largely unknown. We hypothesized that the incidence of atherothrombosis may increase when an additional risk factor for atherothrombosis is introduced on top of the impaired anticoagulant activity by knockdown of protein C. An important risk factor is for the development of atherothrombosis and consequent cardiovascular hospitalization is pulse pressure (10). A transient increase in blood pressure can be achieved in animal models by the administration of phenylephrine (PE), a selective α1-adrenergic receptor agonist. This will increase the strain on atherosclerotic plaques thereby stimulating the risk of plaque rupture and subsequent atherothrombosis. In line, PE administration was associated with increased rupture of p53-treated plaques in *Apoe*$^{-/-}$ mice (11). In the current study we therefore also applied PE treatment to increase the strain on the atherosclerotic plaques and stimulate atherothrombosis incidence in the si*Proc* treated *Apoe*$^{-/-}$ mice. Moreover, we attempted to direct atherothrombosis to the carotid artery by placing perivascular collars, a procedure which induces rapid atherogenesis proximal of the collars (12). This allowed us to investigate the impact of low protein C on plaques at an additional predefined vascular site and of a different origin than the plaques in the aortic root.

## MATERIALS AND METHODS

**Animals**

Female C57BL/6 *Apoe*$^{-/-}$ mice (4-7 weeks old, n=57) were fed a Western-type diet (WTD containing 0.15% cholesterol; Special Diet Services, Sussex, UK). After 6 weeks on WTD, mice received silicone collars around both common carotid arteries, as previously described (11). After 10 weeks on WTD, synthetic siRNA (5 mg/kg; Ambion, Life Technologies, Carlsbad (CA), USA) targeting protein C (si*Proc*, cat. #S72192; n=40), or a control siRNA without a known target in mice (siNEG, cat. #4404020; n=17) was injected intravenously (IV). siRNA was complexed using invivofectamine 3.0, and each mouse received 2.5 nmol siRNA. Prior to siRNA injection, mouse groups were randomized based on weight and age (supplemental table 1). siNEG- and si*Proc*-treated mice received two intravenous injections of either phenylephrine (PE, 8 µg/kg IV, Sigma-Aldrich cat. #P6126-10G, Zwijndrecht, The Netherlands; si*Proc*: n=20, siNEG: n=8) or Phosphate-Buffered Saline (PBS; si*Proc*: n=20, siNEG: n=9) as control. PE or PBS injections were performed 4 and 6 days after the siRNA injection. In both the siNEG and the si*Proc* group, one mouse was removed from the experiment due to procedural errors, and thus not represented in the analyses. For an overview of the experimental procedure, see supplemental figure 1. The animal experimental protocol was in agreement with the national guidelines for animal experimentation and was approved by the Ethics Committee for Animal Experiments (Leiden University, Leiden, The Netherlands).

**Tissue harvesting and preparation**

Seven days after siRNA injection, mice were anesthetized with a subcutaneous injection of a mixture of ketamine (100 mg/kg), xylazine (12.5 mg/kg) and atropine (125 µg/kg). Citrated blood (300 µL) was drawn from the inferior vena cava, and plasma was collected as described previously (13). For whole blood cell and platelet analysis, an EDTA blood sample (approximately 50 µL) was collected through retro-orbital bleeding, upon blood withdrawal from the vena cava. Subsequently, mice were further exsanguinated and perfused *in situ* with PBS, after which organs were harvested. Tissues were either snap frozen (liver and spleen, stored at -80°C), or fixed for 24 hours in 3.7% neutral-buffered formalin (heart and carotid arteries, Formal-Fixx, Shandon Scientific Ltd, UK) and stored at room temperature for analysis.

**Gene expression evaluation**

Transcript of *Proc* was assessed by routinely quantitative PCR of hepatic tissue, with *Actb* as a reference housekeeping gene (14).





**Histology**

Hearts (aortic roots) and carotid arteries were formalin fixed and embedded in OCT compound (Optimum Cutting Temperature; Sakura Finetek Europe B.V., Alphen aan de Rijn, The Netherlands) before sectioning. Cryosections (10mm, 70mm interval) of the aortic root were prepared and mounted in a parallel series on 1% gelatin coated slides. Thrombi and clot structures in the aortic root were identified and scored blindly by two independent researchers on hematoxylin and eosin-stained sections. Plaque size per valve was determined after staining of the cyrosections for neutral lipids using Oil-Red-O and hematoxylin (Sigma-Aldrich, Zwijndrecht, The Netherlands). Corresponding sections were stained using the Masson's Trichrome method (Sigma-Aldrich) for further morphometric analysis of the atherosclerotic plaques, including the percentage of collagen, necrotic core, and macrophage foam cells. All images were analyzed by blinded computer aided morphometric analysis using the Leica DM-RE microscope and LeicaQwin software (Leica Ltd, Cambridge, UK). Transverse serial cryosections (10mm; 80mm interval) of the carotid arteries (and the collars) were made. Sections were routinely stained with hematoxylin and eosin for a general assessment of histology, and were analyzed blindly by two independent researchers.

**Blood and plasma analysis**

Whole blood cell and platelet analysis were performed using an automated XT-2000iV veterinary hematology analyzer (Sysmex Europe GMBH, Norderstedt, Germany). Plasma cholesterol levels were measured by an enzymatic colorimetric assay (Roche diagnostics, Almere, The Netherlands). Protein C plasma levels were determined using an ELISA with a sheep anti-murine protein C polyclonal antibody (Haematologic Technologies Inc. Essex Junction (VT), USA), conjugated with Horseradish peroxidase with the EZ-Link Plus Activated Peroxidase Kit (Thermo Scientific, #31489, Waltham (MA), USA), as described previously (14). Fibrinogen and Serum Amyloid A plasma levels were determined using commercial ELISA kits (Affinity Biologicals, Ancaster (ON), Canada and R&D systems, Minneapolis (MN), USA, respectively).

**Statistics**

Statistical analysis was performed in Graphpad Instat (GraphPad Software, La Jolla (CA), USA). Data are presented with median and range. Statistical differences were assessed using the Mann-Whitney U test. A *P*-value <0.05 was considered significant. Descriptive statistic and calculate proportions of the observations and the 95% confidence intervals (Wilson-score) were calculated using resources provided by the Open Source Epidemiologic Statistics for Public Health website (www.openepi.com). A Chi-Square test was performed for the valve-incidence was done in SPSS (IBM SPSS Statistics for Windows, Version 23.0, Armonk (NY), USA).

## RESULTS

At the time of sacrifice, all *Apoe*$^{-/-}$ mice treated with PBS or with phenylephrine (PE) and siRNA (both siNEG and si*Proc*) appeared healthy and did not show any abnormalities. Histological analysis of the aortic root of 10 weeks WTD-fed si*Proc* treated mice demonstrated the presence of atherosclerotic plaque-associated thrombi, with a similar size and composition as previously reported (9). In total, 9 out of 39 si*Proc* treated *Apoe*$^{-/-}$ mice (23.0%, CI (95%): 16.7-47.9) were categorized as atherothrombosis-positive in the aortic root (figure 1A-D and supplemental figure 2). In addition to the 9 mice with typical plaque-associated thrombi, 2 mice developed atypical clots in the aortic root. One atypical clot, although fibrin-positive and clearly associated with an atherosclerotic plaque, did not have the layered structure and did not contain leukocytes as the typical thrombi. These are histological arguments for being a fresh thrombus (supplemental figure 3A). The second atypical thrombus was associated with a valve, although present in the aortic sinus. Despite its unusual location, the thrombus was similar to the typical thrombi found on top of the atherosclerotic plaques. The valve with which it was associated contained a high number of leukocytes, but this was not unique for this specific heart valve (supplemental figure 3B). Both thrombi were not included in further analyses of the thrombus-positive group.

To investigate if an additional predefined site allowing atherothrombosis development could be created, perivascular collars were placed around both the carotid arteries of the *Apoe*$^{-/-}$ mice, 4 weeks prior to siRNA treatment. In line with previous studies (12, 15), histological analysis of the carotid arteries showed that collar placement resulted in maximum atherosclerotic plaque formation proximal to the collar. Although gross visual inspection revealed a large variation in plaque size and composition within groups, these were not different at the site of maximal stenosis between mice in the different groups (supplemental figure 4). In total, 1 out of 39 si*Proc* mice presented a structure identified as a thrombus in one of the carotid arteries (figure 1E-F). The thrombus was associated with the plaque, was rich in erythrocytes, and had a layered structure, comparable to the thrombi found in the aortic root. siNEG treated mice did not show events or structures identified as thrombus, neither in the aortic root and nor in the carotid arteries. It should however be noted that in our long term experience with collar placement around the carotid arteries of *Apoe*$^{-/-}$ mice, the occurrence of thrombosis as a complication of the procedure is not a rare event. Silencing of *Proc* induced atherothrombosis does seems to be restricted to the aortic root.

Livers and blood/plasma were analyzed to determine whether specific markers could be correlated to atherothrombosis susceptibility. As expected, si*Proc* treatment strongly decreased hepatic *Proc* transcript levels, compared to siNEG treated mice (remaining *Proc* transcript: mice without thrombi (-THR): 32.0% (18.0-63.7), mice with thrombi (+THR): 25.8% (18.8-40.0), $P<0.001$,





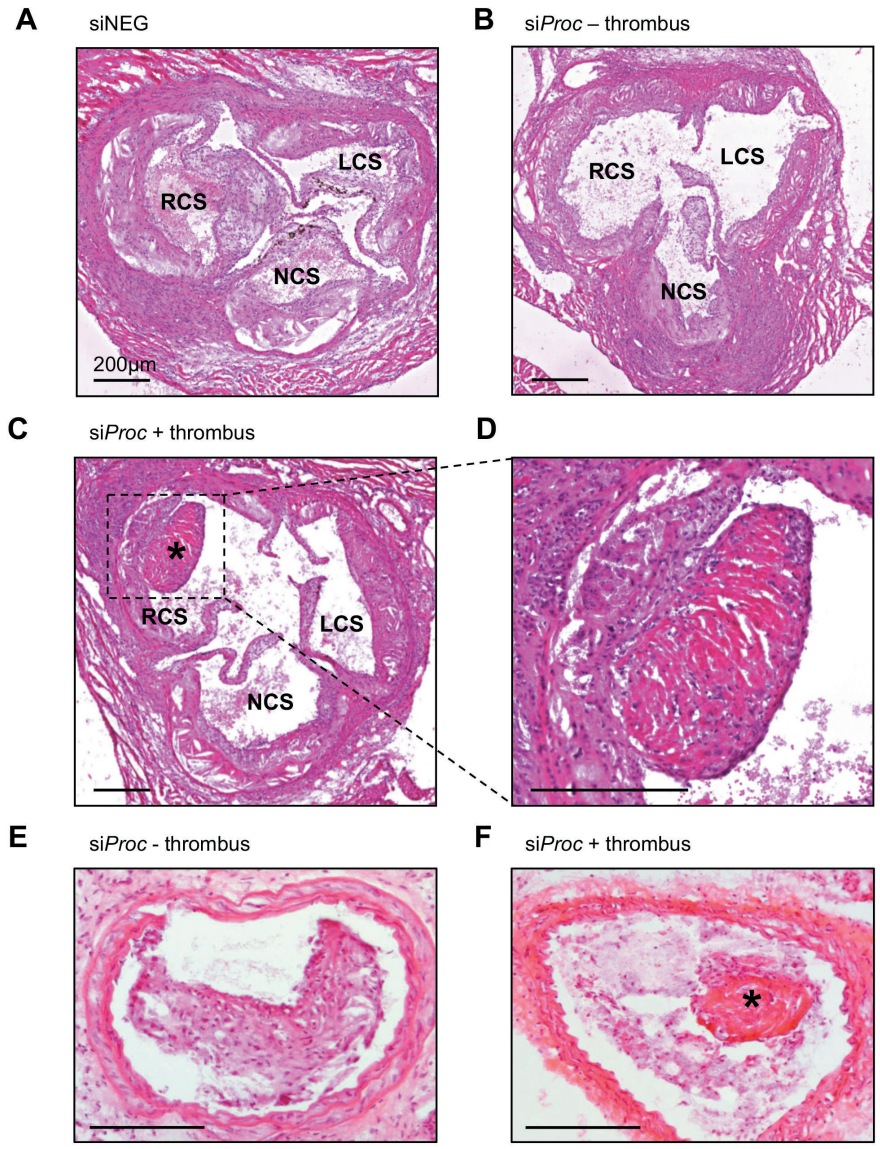


**Figure 1 | Atherothrombosis in the aortic root of si*Proc* treated *Apoe*$^{-/-}$ mice.** (A) Representative section of the aortic root of a mouse treated with siNEG. (B) Representative section of the aortic root of a mouse treated with si*Proc*, without a thrombus. (C and D) Representative section of the aortic root of a mouse treated with si*Proc*, with a thrombus associated with an atherosclerotic plaque. (E) Representative section of the common carotid artery containing an atherosclerotic lesion upon collar placement, derived from an si*Proc* treated mouse. (F) A thrombus-like structure associated with an atherosclerotic lesion in the common carotid artery. All sections are hematoxylin and eosin (HE) stained. NCS: Non-coronary sinus, RCS: Right coronary sinus, LCS: Left coronary sinus. *: Thrombus. Black bars represent 200 µm.
si*Proc* mice treated with PE had a similar incidence of atherothrombosis compared to PBS-treated si*Proc* mice (4 out of 19 vs. 5 out of 20 mice, respectively, supplemental figure 2).

figure 2A). Interestingly, the *Proc* transcript in si*Proc* treated mice was significantly lower in mice that presented with atherothrombosis, compared to the mice without atherothrombosis (*P*=0.013, figure 2A). Protein C plasma levels were also reduced in si*Proc* treated mice, as compared to the siNEG treated mice (remaining plasma protein C: -THR: 49.4% (18.4-118.7), +THR: 40.5% (33.2-50.3), *P*<0.001, figure 2B). However, in contrast to the *Proc* transcript data, protein C plasma levels did not reach statistical significance between si*Proc* treated mice with and without a thrombus (*P*=0.11, figure 2B).

Blood cell counts (total white blood cells, neutrophils, lymphocytes, monocytes, eosinophils, and red blood cells) were comparable between siNEG and si*Proc* treated mice with or without atherothrombosis (supplemental figure 6). Interestingly, platelet levels were significantly higher in si*Proc* treated mice compared to siNEG treated mice (-THR: 1280x$10^9$/L (728-1632), +THR: 1512x$10^9$/L (1004-1696), *P*<0.001, figure 2C). Within the si*Proc* treated groups, mice with atherothrombosis had even more platelets (*P*=0.043, figure 2C). To follow-up on this observation, we determined mRNA levels in the spleen of genes associated with platelet production. In agreement with the increased platelet counts, upon si*Proc* treatment, expression of some of these genes (*Gata1*, *Itga2b*, *Nfe2*, and *Fog1*) were increased as compared to siNEG treated mice (data not shown). si*Proc* treated mice with a thrombus showed an increased expression for *Fog1*, while for the other spleen-expressed genes expression levels were not different between mice with and without a thrombus.

Plasma analysis showed that total cholesterol levels were not significantly different between mice treated with siNEG or si*Proc,* with or without atherothrombosis (siNEG: 10.1 mg/mL (5.4-11.9), si*Proc* -THR: 9.5 mg/mL (6.4-12.8), si*Proc* +THR: 10.1 mg/mL (9.1-13.9), *P*=0.43, figure 2D). Besides total cholesterol, fibrinogen and serum amyloid A (SAA, an acute-phase mouse protein associated with inflammation (16)) were determined as possible systemic markers for atherothrombosis susceptibility. In line with fibrinogen being a cardiovascular risk factor in epidemiological studies (17), plasma fibrinogen levels in all groups of *Apoe*$^{-/-}$ mice were significantly higher than levels measured in normal pool plasma (NPP, pool of C57BL/6 mouse plasma). However, among siRNA treated *Apoe*$^{-/-}$ mice no differences were observed (siNEG: 363% (83-598), si*Proc* -THR: 394% (35-562), si*Proc* +THR: 463% (2.6-564), *P*=0.74, figure 2E). SAA levels were slightly increased in plasma of the *Apoe*$^{-/-}$ mice compared to NPP (<0.5 ng/mL), but no differences among the *Apoe*$^{-/-}$ groups were found (siNEG: 0.90 ng/mL (0.40-3.04), si*Proc* -THR: 1.29 ng/mL (0.41-3.12), si*Proc* +THR: 0.80 ng/mL (0.51-3.78), *P*=0.33, figure 2F). In line with the previous results, PE treatment did not influence plasma levels of any of the measured parameters (supplemental figure 7).

In our previous study, we found no significant correlation between plaque size and phenotype and the susceptibility to aortic root atherothrombosis, but with only 4 mice displaying athero-





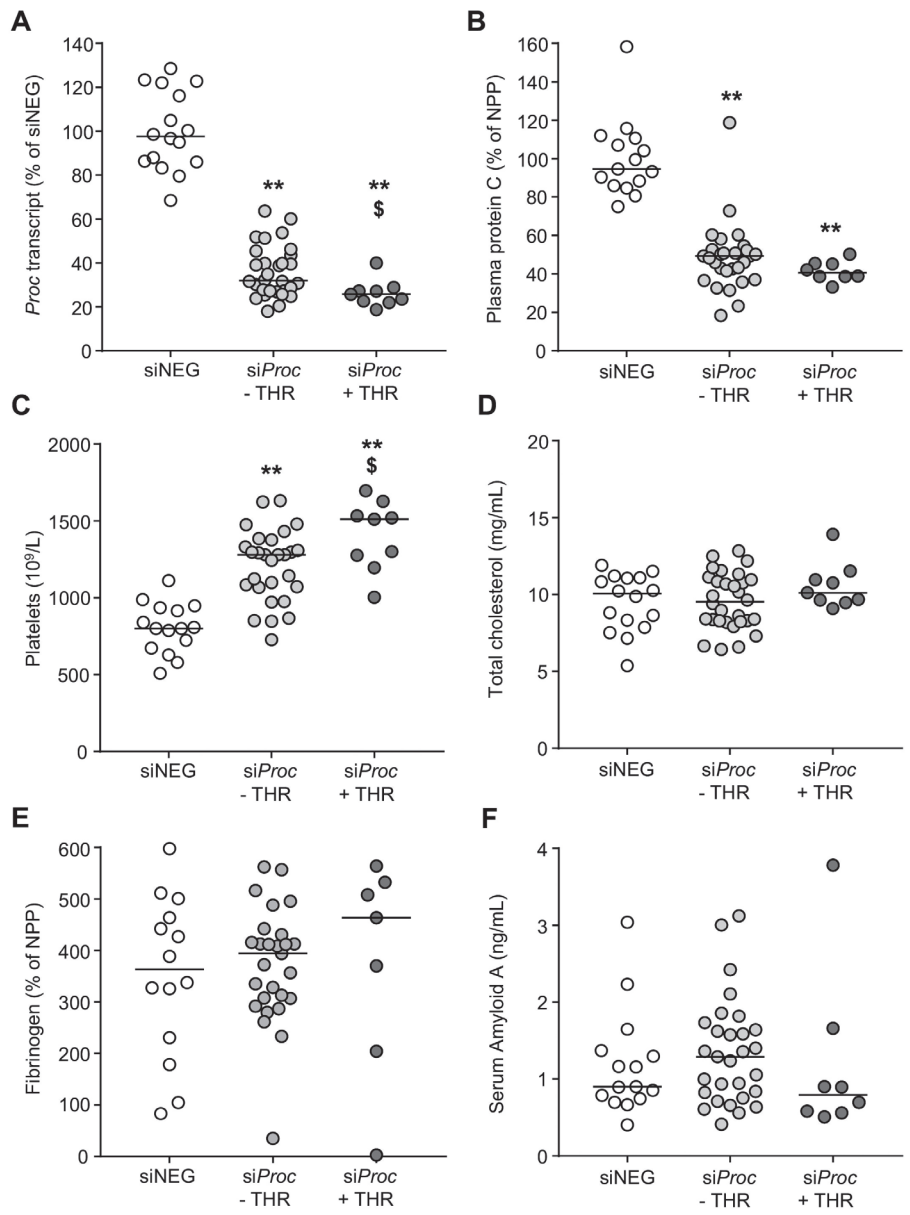


**Figure 2 | Liver, blood, and plasma analysis of siNEG and si*Proc* treated *Apoe*$^{-/-}$ mice.** (A) *Proc* transcript in the liver upon sacrifice (7 days after si*Proc* treatment) compared to the mean value of siNEG treated mice (100%), (B) Plasma protein C levels, measured by ELISA, compared to the mean value of siNEG treated (100%), (C) Total blood platelet levels, (D) Plasma total cholesterol levels, (E) Plasma fibrinogen levels, measured by ELISA, and expressed as % of normal pool plasma. We did not have any reason to exclude outliers with a low value (e.g. due to coagulation upon blood withdrawal), (F) Serum Amyloid A levels. Black bars indicate the median. *: *P*<0.05, **: *P*<0.01 for siNEG vs. si*Proc*. $: *P*<0.05 for si*Proc* –THR vs. si*Proc* +THR.

thrombosis the power in that study was low (9). Therefore, in the current study the atherosclerotic plaques in the aortic root were also morphometrically analyzed to assess whether plaque size and characteristics could be linked to the presence of atherothrombosis (for examples of plaque stainings, see figures 3A and 3B). Plaque analysis revealed that PE treatment, similar to the atherothrombosis incidence, did not influence any of the plaque characteristics (supplemental figure 5). For this reason, data of the mice with and without PE treatment were pooled to increase statistical power. In the si*Proc* groups, the plaque area (without thrombus (-THR): 191x$10^3$ µm$^2$ (55.0-888), +THR: 191x$10^3$ µm$^2$ (112-343), *P*=0.59, figure 3C), were not different. Interestingly, collagen and macrophage content were significantly lower in plaques with an associated thrombus (-THR: 13.4% (2.1-29.6), +THR: 8.3% (6.4-15.3), *P*=0.031, figure 3D, and -THR: 9.1% (0.8-34.9), +THR: 6.7% (4.5-13.7), *P*=0.028, figure 3E, respectively), unlike the necrotic core (-THR: 19.5% (4.3-80.2), +THR: 15.3% (7.8-67.0), *P*=0.30, figure 3F). No evidence was found for the occurrence of intraplaque hemorrhages or other abnormalities in the atherosclerotic plaques (with or without superimposed thrombi).

Since in our studies thrombi were exclusively found in the aortic root, we hypothesized that local hemodynamics, which can influence endothelial integrity, plays a role in atherothrombosis formation. For this reason, we re-examined the individual plaques formed in the different cusps within the aortic root (sinuses) for the presence of thrombi, by dividing the aortic root into the left coronary sinus (LCS), right coronary sinus (RCS), and non-coronary sinus (NCS, see (18-20) and figure 4A). We noticed that thrombi had a preference for the RCS, over the LCS and the NCS (figure 4B, *P*=0.018). When combining these data with the data obtained from our previous study, where we detected 4 atherothrombosis events for in total 29 si*Proc* injected *Apoe*$^{-/-}$ (9), the preference for the RCS was even more pronounced (*P*=0.008). To exclude that the predilection for the RCS was the consequence of differences in plaque size and composition, the plaque parameters were reanalyzed for the LCS, NCS, and RCS, but no significant differences among plaques were found (supplemental figure 8).

## DISCUSSION

Transgenic mice with an impaired lipoprotein metabolism, such as *Apoe*$^{-/-}$ and *Ldlr*$^{-/-}$ mice, which are fed a cholesterol-rich diet rapidly develop advanced atherosclerosis (1, 2). However, in contrast to humans, these mice only develop atherothrombotic events upon additional (invasive) plaque damaging interventions (21). The cause for the absence of atherothrombosis is unknown, but it is likely that multiple species-specific factors such as hemodynamics, plaque composition, metabolism, and life span are involved (22). Recently, our group showed that transient lowering of the natural anticoagulant protein C in *Apoe*$^{-/-}$ mice resulted in spontaneous atherothrombosis





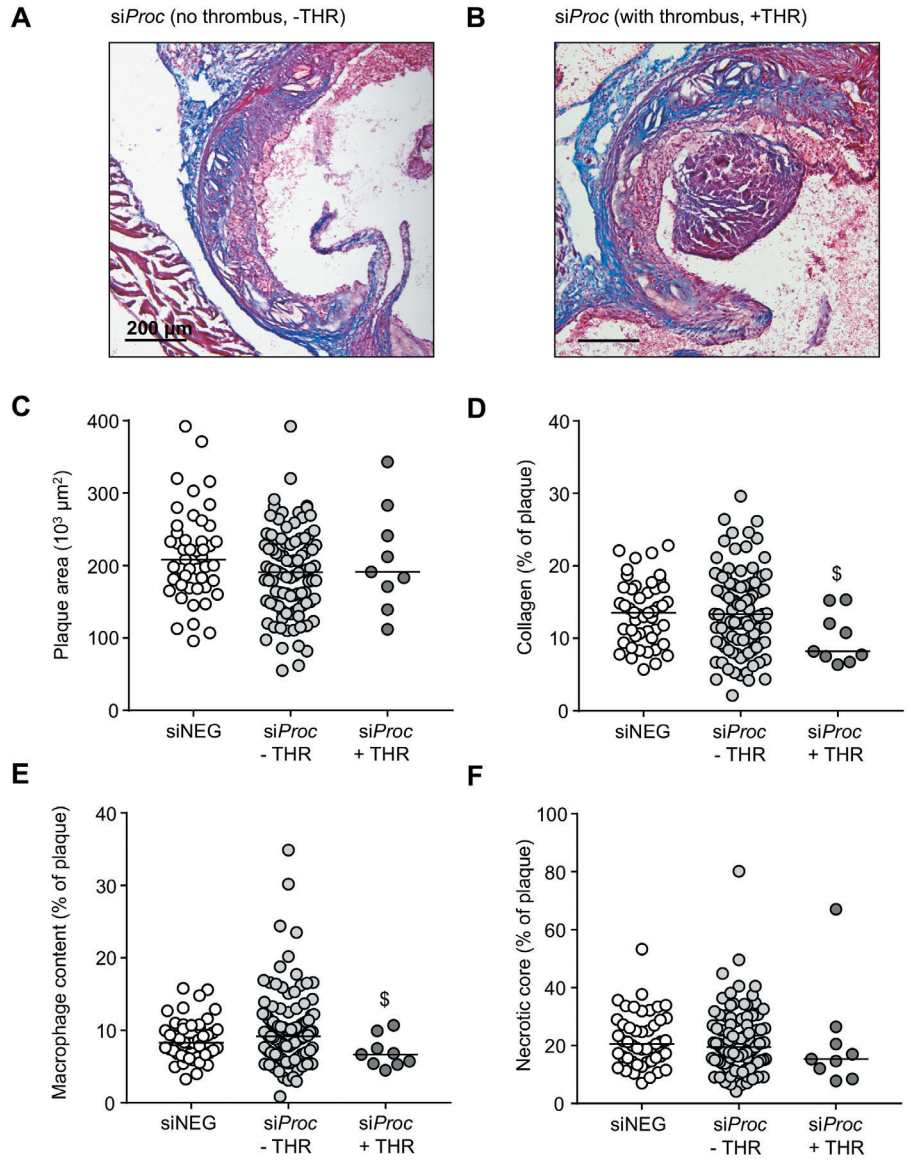


**Figure 3 | Plaque composition of siNEG and si*Proc* treated *Apoe*$^{-/-}$ mice.** (A-B) Representative photo-micrograph of a Masson's Trichrome stained plaque in the aortic root (RCS) of mice treated with si*Proc*, without (A) and with (B) a thrombus associated to a plaque from the aortic root. Blue areas were assessed as collagen-positive, non-stained areas as necrotic core, and pink nucleated areas as macrophage content/ foam cells. Black bars represent 200 µm. (C-F) Individual plaques from the si*Proc* treated group are divided in plaques without a thrombus (si*Proc* –THR) and plaques containing a thrombus (si*Proc* +THR). (A) Total plaque area, (B) Collagen, (C) Cellular content, (D) Necrotic core. For all panels, the indicated values represent an average measurement of three sections. Black bars indicate the median. $: *P*<0.05 for si*Proc* –THR vs. si*Proc* +THR.

**A**

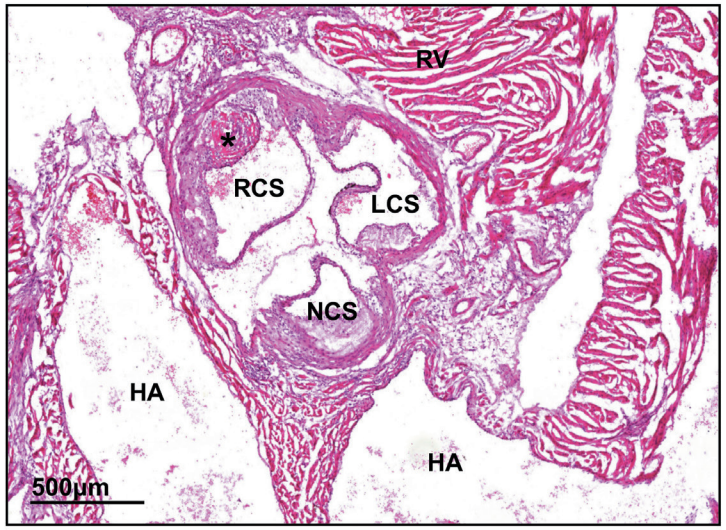


**B**

| Study | LCS | NCS | RCS |
|---|---|---|---|
| Ouweneel et al. | 0 | 2 | 3 |
| | LCS | NCS | RCS |
| Current | 1 | 1 | 7* |
| | LCS | NCS | RCS |
| Overall | 1 | 3 | 10** |

**Figure 4 | si*Proc* induced atherothrombosis in the different sinuses of the aortic root of *Apoe*$^{-/-}$ mice.** (A) HE stained section of the aortic root and surrounding tissues. The non-coronary sinus (NCS) of the aortic root is covered by the two atria of the heart (atria are indicated with HA). Left and right of the NCS the left and right coronary sinuses (LCS and RCS, respectively) are present, which are both partly covered by a muscle-rich area, from which the largest part is the right ventricle (indicated with RV). *: thrombus. Black bar represents 500 µm. (B) Overview of three independent studies, where atherothrombosis in the aortic root occurred upon si*Proc* treatment. *: $P<0.05$, **: $P<0.01$.





at plaques formed in the sinuses of the aortic root (9). This implies that potent anticoagulation (co)contributes to absence of atherothrombosis in mice. In the current study we aimed to increase the insight into the factors which associate and possibly determine when and where a thrombus develops on top of an atherosclerotic plaque. For the first time we provide evidence that atherosclerotic plaques located in the right coronary sinus of the aortic root (RCS) are more prone to the development of atherothrombosis, compared to the other two sinuses (left and non-coronary sinuses, LCS and NCS, respectively). Interestingly, plaques with a thrombus were modestly but significantly lower in collagen and macrophage content. Therefore, we conclude that low protein C-induced atherothrombosis in mice is a low incident but reproducible phenomenon, and that it is determined by the location of the plaque, possibly in combination with differences in plaque composition.

Since Leonardo da Vinci in the beginning of the XVI century, scientists have been intrigued by the sophisticated and sustainable tissue and milieu of the aortic valves and root (23-25). The mouse aortic sinuses (in humans, sinuses of Valsalva), play a crucial role in regulating the closing mechanism of the valve leaflets (26). The oscillating shear stress due to the opening and closing of the valves render the cusps susceptible for the development of atherosclerotic plaques. A limited number of studies have distinguished between the three different sinuses and their plaques during their analyses. It has been reported that plaque size is reduced specifically in the RCS upon treatment with two different liver X receptor agonists (19). This means that differences in local anatomy of the aortic root do not only cause the flow to be different, but also can induce different expression patterns of proteins, possibly linked to coagulation. Moreover, Bentzon et al. suggested a causal relation between lesion formation and expansive remodeling of the aortic root sinuses, which was different when comparing plaques in the NCS, LCS, and RCS (27). The observed sinus preference for the development of atherothrombosis suggests that in mice local hemodynamics and wall shear stress are not only involved in atherogenesis (28, 29), but also in the development of atherothrombosis, as has been proposed for the human disease (30, 31). The identification of factors that drive the predilection for the RCS may provide novel clues on factors that drive atherothrombosis in mice and humans.

Plaques in the aortic root which were associated with a thrombus appeared to be lower in macrophage and collagen content. Although the measured values fell within the normal range, the difference was considered statistically different. Macrophages (foam cells) are crucially involved in atherogenesis and a high content of this cell population within a plaque has been associated with instability (32, 33). These observations make our findings in the current study, where in atherothrombotic plaques relatively fewer macrophages were found, unexpected. However, it should be noted that the plaques were advanced and that as a result the macrophage foam cell content was low. It has been described that lower collagen levels in atherosclerotic plaques

are associated with instability and risk of rupture (34). However, because of the current study setup, we cannot conclude whether the observed difference is a cause or consequence of the formation of a thrombus.

In the current study, si*Proc* treatment of *Apoe*$^{-/-}$ mice increased platelet levels, likely due to increased platelet production. A similar increase in platelet numbers was observed in the absence of an atherosclerotic phenotype in an independent experiment in which wild type female C57BL/6 mice on a normal chow diet were treated with an siRNA against *Proc* (data not shown). These findings suggest that the anticoagulant protein C directly or indirectly influences platelet production (and possibly consumption and/or clearance), a phenomenon that, to our knowledge, has not been described before. In human studies, it has been suggested that increased platelet levels are a risk factor for atherothrombotic events, making it tempting to speculate that the higher platelet levels upon si*Proc*-treatment contribute to the development of atherothrombosis in the aortic root (35, 36). For now, it is however not clear whether the increased platelets predict aortic root atherothrombosis susceptibility or whether they are a consequence of the event.

In conclusion, atherosclerotic plaques in the RCS are a predilection site for low protein C-induced spontaneous atherothrombosis in *Apoe*$^{-/-}$ mice, a process associated with vulnerable plaques displaying a lower macrophage and collagen content and vulnerable blood with augmented platelet counts.

## ACKNOWLEDGEMENTS

The authors thank Dr. I. Bot for technical assistance with the collar operations and for critical reading of the manuscript.





## REFERENCES


1. Zhang SH, Reddick RL, Piedrahita JA, Maeda N. Spontaneous hypercholesterolemia and arterial lesions in mice lacking apolipoprotein E. *Science.* 1992;258(5081):468-71.
2. Ishibashi S, Brown MS, Goldstein JL, Gerard RD, Hammer RE, Herz J. Hypercholesterolemia in low density lipoprotein receptor knockout mice and its reversal by adenovirus-mediated gene delivery. *J Clin Invest.* 1993;92(2):883-93.
3. Veniant MM, Withycombe S, Young SG. Lipoprotein size and atherosclerosis susceptibility in *Apoe*$^{(-/-)}$ and Ldlr$^{(-/-)}$ mice. *Arterioscler Thromb Vasc Biol.* 2001;21(10):1567-70.
4. Veniant MM, Beigneux AP, Bensadoun A, Fong LG, Young SG. Lipoprotein size and susceptibility to atherosclerosis--insights from genetically modified mouse models. *Curr Drug Targets.* 2008;9(3):174-89.
5. Getz GS, Reardon CA. Do the *Apoe*$^{-/-}$ and Ldlr$^{-/-}$ Mice Yield the Same Insight on Atherogenesis? *Arterioscler Thromb Vasc Biol.* 2016;36(9):1734-41.
6. Libby P, Pasterkamp G. Requiem for the 'vulnerable plaque'. *Eur Heart J.* 2015;36(43):2984-7.
7. Matoba T, Sato K, Egashira K. Mouse models of plaque rupture. *Curr Opin Lipidol.* 2013;24(5):419-25.
8. Lippi G, Franchini M, Targher G. Arterial thrombus formation in cardiovascular disease. *Nat Rev Cardiol.* 2011;8(9):502-12.
9. Ouweneel AB, Heestermans M, Verwilligen RAF, Gijbels MJJ, Reitsma PH, Van Eck M, et al. Silencing of Anticoagulant Protein C Evokes Low-Incident but Spontaneous Atherothrombosis in Apolipoprotein E-Deficient Mice-Brief Report. *Arterioscler Thromb Vasc Biol.* 2017;37(5):782-5.
10. Selvaraj S, Steg PG, Elbez Y, Sorbets E, Feldman LJ, Eagle KA, et al. Pulse Pressure and Risk for Cardiovascular Events in Patients With Atherothrombosis: From the REACH Registry. *J Am Coll Cardiol.* 2016;67(4):392-403.
11. von der Thusen JH, van Vlijmen BJ, Hoeben RC, Kockx MM, Havekes LM, van Berkel TJ, et al. Induction of atherosclerotic plaque rupture in apolipoprotein E$^{-/-}$ mice after adenovirus-mediated transfer of p53. *Circulation.* 2002;105(17):2064-70.
12. von der Thusen JH, van Berkel TJ, Biessen EA. Induction of rapid atherogenesis by perivascular carotid collar placement in apolipoprotein E-deficient and low-density lipoprotein receptor-deficient mice. *Circulation.* 2001;103(8):1164-70.
13. Safdar H, Cheung KL, Vos HL, Gonzalez FJ, Reitsma PH, Inoue Y, et al. Modulation of mouse coagulation gene transcription following acute in vivo delivery of synthetic small interfering RNAs targeting HNF4alpha and C/EBPalpha. *PLoS One.* 2012;7(6):e38104.

14. Safdar H, Cheung KL, Salvatori D, Versteeg HH, Laghmani el H, Wagenaar GT, et al. Acute and severe coagulopathy in adult mice following silencing of hepatic antithrombin and protein C production. *Blood.* 2013;121(21):4413-6.

15. Bot M, Bot I, Lopez-Vales R, van de Lest CH, Saulnier-Blache JS, Helms JB, et al. Atherosclerotic lesion progression changes lysophosphatidic acid homeostasis to favor its accumulation. *Am J Pathol.* 2010;176(6):3073-84.

16. Uhlar CM, Whitehead AS. Serum amyloid A, the major vertebrate acute-phase reactant. *Eur J Biochem.* 1999;265(2):501-23.

17. Ernst E, Resch KL. Fibrinogen as a cardiovascular risk factor: a meta-analysis and review of the literature. *Ann Intern Med.* 1993;118(12):956-63.

18. Icardo JM, Colvee E. Origin and course of the coronary arteries in normal mice and in iv/iv mice. *J Anat.* 2001;199(Pt 4):473-82.

19. Peng D, Hiipakka RA, Reardon CA, Getz GS, Liao S. Differential anti-atherosclerotic effects in the innominate artery and aortic sinus by the liver X receptor agonist T0901317. *Atherosclerosis.* 2009;203(1):59-66.

20. de Kerchove L, Jashari R, Boodhwani M, Duy KT, Lengele B, Gianello P, et al. Surgical anatomy of the aortic root: implication for valve-sparing reimplantation and aortic valve annuloplasty. *J Thorac Cardiovasc Surg.* 2015;149(2):425-33.

21. Kuijpers MJ, Gilio K, Reitsma S, Nergiz-Unal R, Prinzen L, Heeneman S, et al. Complementary roles of platelets and coagulation in thrombus formation on plaques acutely ruptured by targeted ultrasound treatment: a novel intravital model. *J Thromb Haemost.* 2009;7(1):152-61.

22. Tchaikovski SN, BJ VANV, Rosing J, Tans G. Development of a calibrated automated thrombography based thrombin generation test in mouse plasma. *J Thromb Haemost.* 2007;5(10):2079-86.

23. Bissell MM, Dall'Armellina E, Choudhury RP. Flow vortices in the aortic root: in vivo 4D-MRI confirms predictions of Leonardo da Vinci. *Eur Heart J.* 2014;35(20):1344.

24. De Paulis R, Salica A, Pisani G, Morbiducci U, Weltert L, Maselli D. Hemodynamics of the aortic valve and root: implications for surgery. *Ann Cardiothorac Surg.* 2013;2(1):40-3.

25. Robicsek F. Leonardo da Vinci and the sinuses of Valsalva. *Ann Thorac Surg.* 1991;52(2):328-35.

26. Bellhouse BJ, Bellhouse FH, Reid KG. Fluid mechanics of the aortic root with application to coronary flow. *Nature.* 1968;219(5158):1059-61.

27. Bentzon JF, Pasterkamp G, Falk E. Expansive remodeling is a response of the plaque-related vessel wall in aortic roots of apoE-deficient mice: an experiment of nature. *Arterioscler Thromb Vasc Biol.* 2003;23(2):257-62.





28. Zhu H, Zhang J, Shih J, Lopez-Bertoni F, Hagaman JR, Maeda N, et al. Differences in aortic arch geometry, hemodynamics, and plaque patterns between C57BL/6 and 129/SvEv mice. *J Biomech Eng.* 2009;131(12):121005.

29. VanderLaan PA, Reardon CA, Getz GS. Site specificity of atherosclerosis: site-selective responses to atherosclerotic modulators. *Arterioscler Thromb Vasc Biol.* 2004;24(1):12-22.

30. Arroyo LH, Lee RT. Mechanisms of plaque rupture: mechanical and biologic interactions. *Cardiovasc Res.* 1999;41(2):369-75.

31. Chen YC, Huang AL, Kyaw TS, Bobik A, Peter K. Atherosclerotic Plaque Rupture: Identifying the Straw That Breaks the Camel's Back. *Arterioscler Thromb Vasc Biol.* 2016;36(8):e63-72.

32. Moore KJ, Sheedy FJ, Fisher EA. Macrophages in atherosclerosis: a dynamic balance. *Nat Rev Immunol.* 2013;13(10):709-21.

33. Moore KJ, Tabas I. Macrophages in the pathogenesis of atherosclerosis. *Cell.* 2011;145(3):341-55.

34. Hansson GK, Libby P, Tabas I. Inflammation and plaque vulnerability. *J Intern Med.* 2015;278(5):483-93.

35. Elliott MA, Tefferi A. Thrombosis and haemorrhage in polycythaemia vera and essential thrombocythaemia. *Br J Haematol.* 2005;128(3):275-90.

36. Kumagai N, Mitsutake R, Miura S, Kawamura A, Takamiya Y, Nishikawa H, et al. Acute coronary syndrome associated with essential thrombocythemia. *J Cardiol.* 2009;54(3):485-9.

**Supplemental table 1 | Group sizes, age, and body weight for all *Apoe*$^{-/-}$ mice.** For age and body weight, the median and range is displayed of both parameters before siRNA injection. There were no significant differences between groups.

| Group | Group size (n) | Age (weeks) | Body weight (g) |
|---|---|---|---|
| siNEG | 17 | 14 (13-16) | 22.5 (20.9-27.9) |
| si*Proc* | 40 | 14 (13-16) | 22.7 (20.1-25.7) |
| siNEG + PBS | 9 | 14 (13-16) | 22.4 (20.9-27.9) |
| siNEG + PE | 8 | 15 (13-15) | 22.9 (22.1-24.2) |
| si*Proc* + PBS | 20 | 14 (13-16) | 22.6 (20.3-24.9) |
| si*Proc* + PE | 20 | 14 (13-16) | 22.8 (20.1-25.7) |

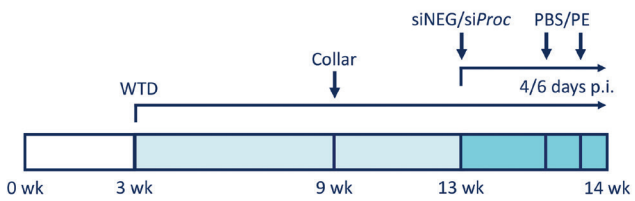


**Supplemental figure 1 | Experimental setup.** 4-7 weeks old female *Apoe*$^{-/-}$ mice were fed a Western type diet (WTD) for 10 weeks. After 6 weeks of WTD, perivascular collars were placed around the common carotid arteries (left and right). After 10 weeks of WTD, mice were treated with either siNEG or si*Proc*. 4 and 6 days after siRNA treatment (post-injection, p.i.), mice were injected with PBS control or phenylephrine (PE). One week after siRNA treatment (age: 15-18 weeks), mice were sacrificed.





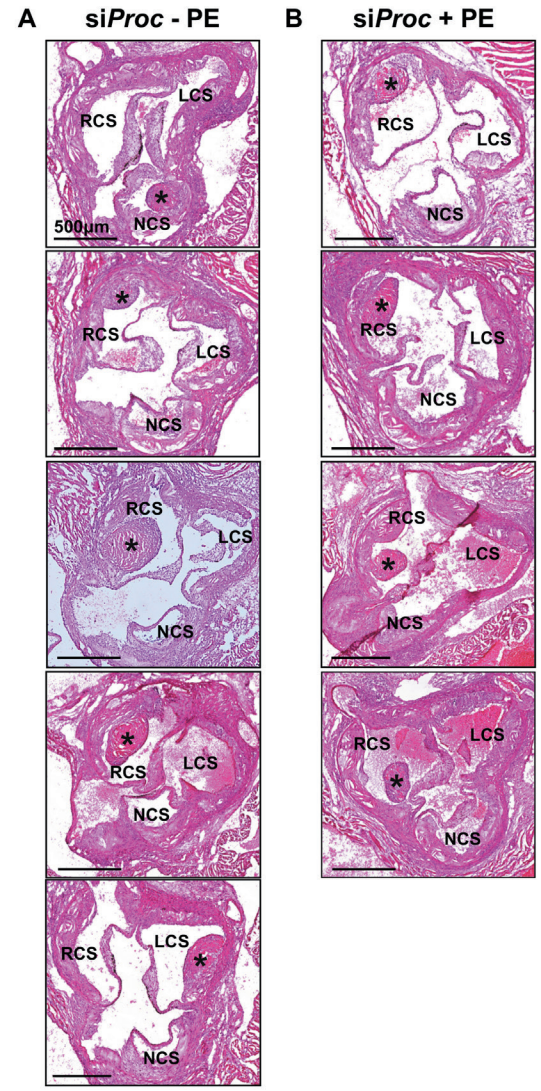


**Supplemental figure 2 | Overview of all si*Proc* associated atherothrombotic events in the aortic root of *Apoe*$^{-/-}$ mice.** (A) In 5 mice in the si*Proc* group without phenylephrine (- PE) treatment atherothrombosis in the aortic root was observed. (B) In 4 mice in the si*Proc* group with phenylephrine (- PE) treatment atherothrombosis in the aortic root was observed. All sections were HE stained. Black bars represent 500 µm. NCS: Non-coronary sinus, RCS: Right coronary sinus, LCS: Left coronary sinus. *: Thrombus.

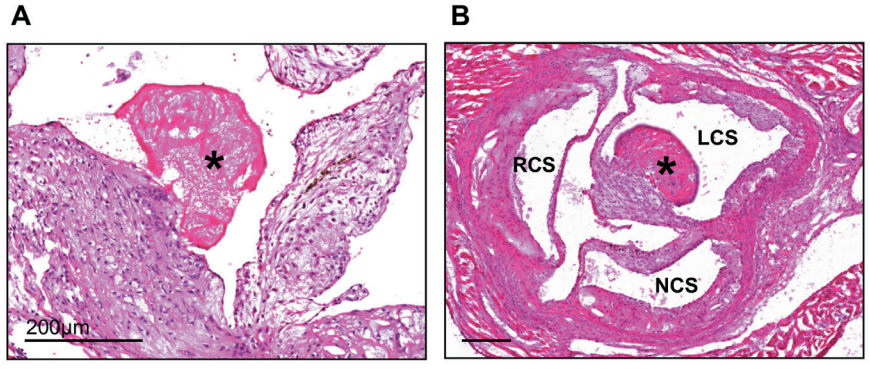


**Supplemental figure 3 | Atypical thrombi in the aortic root of si*Proc* treated *Apoe*$^{-/-}$ mice.** (A) Atypical thrombus which associated with an atherosclerotic plaque. In contrast to other thrombi, it did not have a layered structure and did not contain leukocytes. (B) Atypical thrombus associated with a valve within a sinus of the aortic root, and not with the atherosclerotic plaque. The composition of the thrombus was similar to other thrombi. Both mice were included in the analysis in the si*Proc* group without a thrombus (-THR). Black bars represent 200 µm. NCS: Non-coronary sinus, RCS: Right coronary sinus, LCS: Left coronary sinus. *: Thrombus.





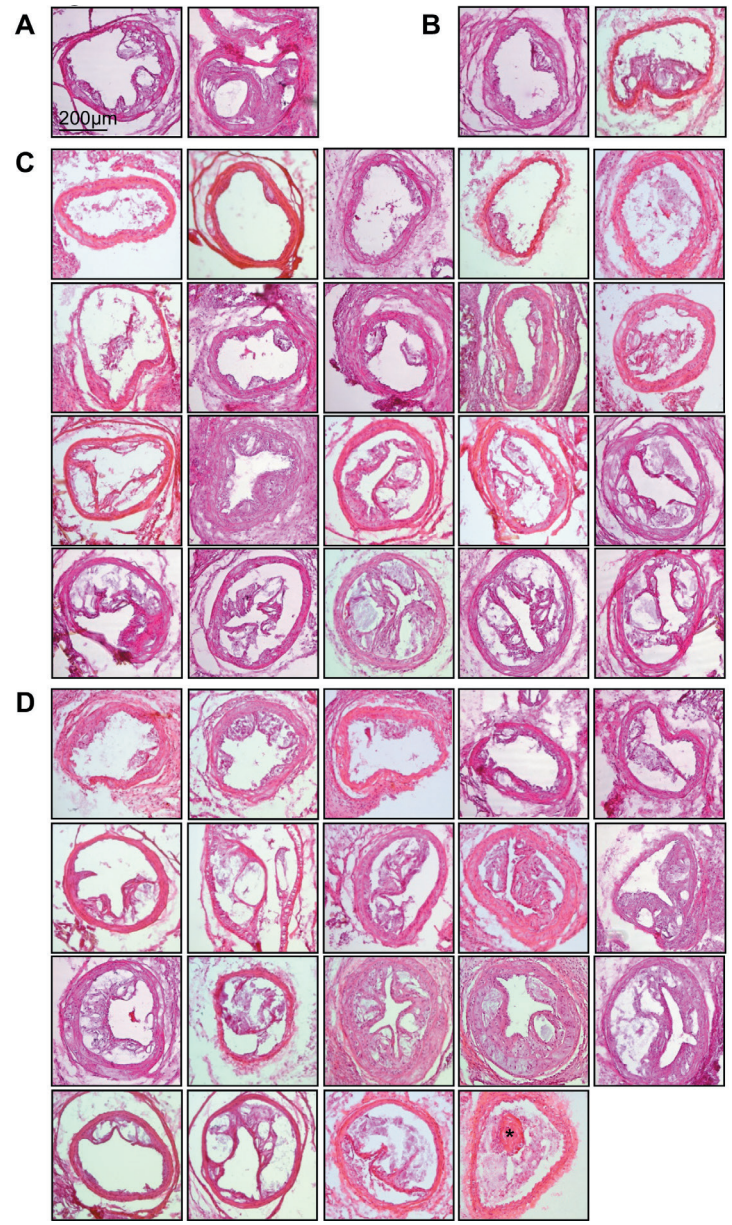


**Supplemental figure 4 | Thrombosis-associated with atherosclerotic plaques upon collar placement in the common carotid arteries.** Overview of sectioned common carotid arteries, at the site of maximal stenosis. (A) Two representative sections of common carotid arteries of mice treated with siNEG (- PE), (B) Two representative sections of common carotid arteries of mice treated with siNEG (+ PE), (C) Sections of common carotid arteries of mice treated with si*Proc* (- PE), (D) Sections of common carotid arteries of mice treated with si*Proc* (+ PE). All sections were HE stained. Black bar represents 200 µm. *: Thrombus (for enlargement, see figure 1F).

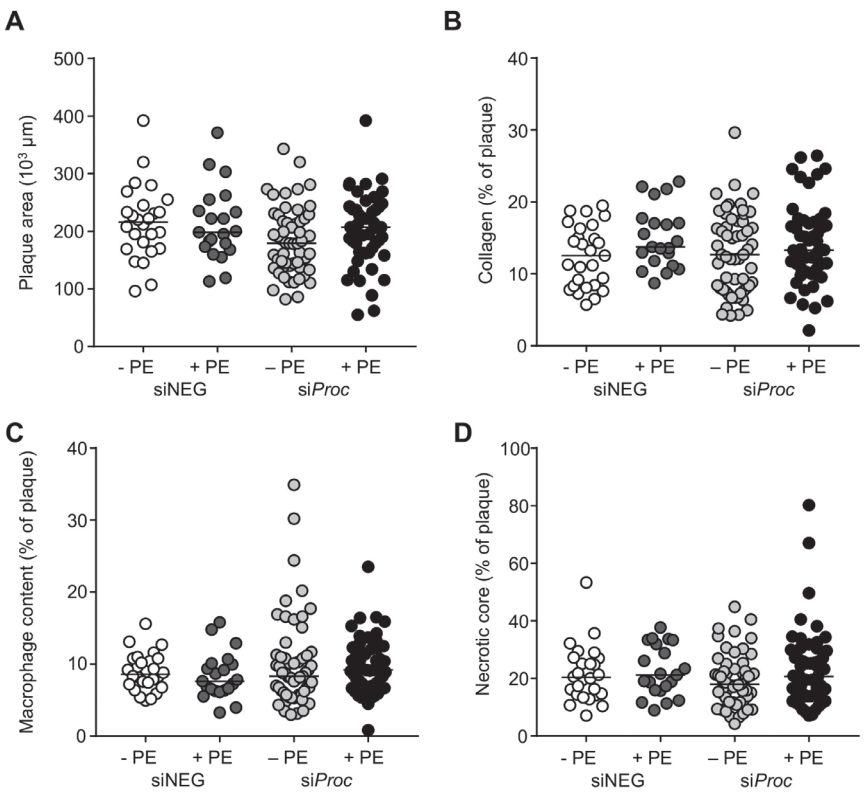


**Supplemental figure 5 | Atherosclerotic plaque composition of siNEG and si*Proc* treated *Apoe*$^{-/-}$ mice, with and without phenylephrine (PE).** (A) Total plaque area, (B) Collagen, (C) Macrophage content, (D) Necrotic core. For all panels, the indicated values represent an average measurement of three sections. Black bars indicate the median.





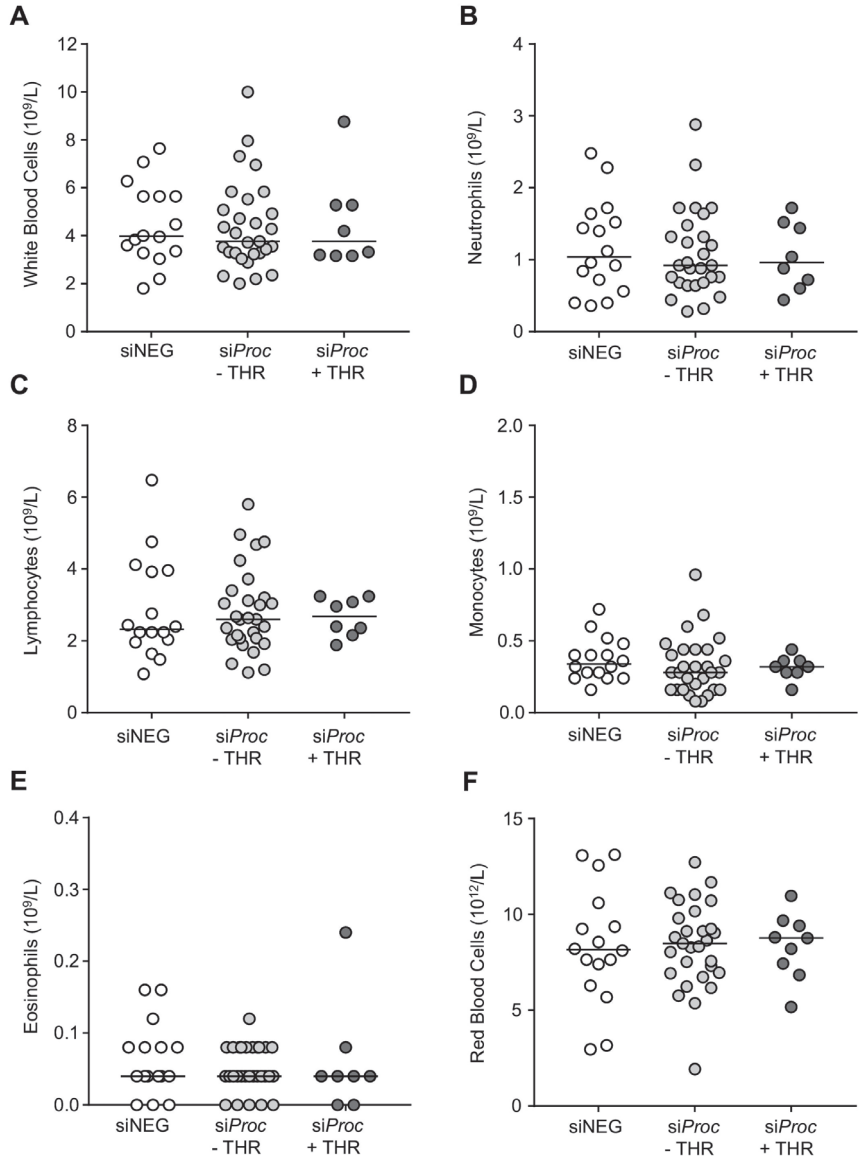


**Supplemental figure 6 | Blood cell populations of siNEG and si*Proc* treated *Apoe*$^{-/-}$ mice.** Blood cell numbers from the si*Proc* treated group is divided in plaques without a thrombus (si*Proc* – THR) and plaques containing a thrombus (si*Proc* +THR). (A) Total white blood cells, (B) Neutrophils, (C) Lymphocytes, (D) Monocytes, (E) Eosinophils, and (F) Red blood cells are displayed. Black bars indicate the median.

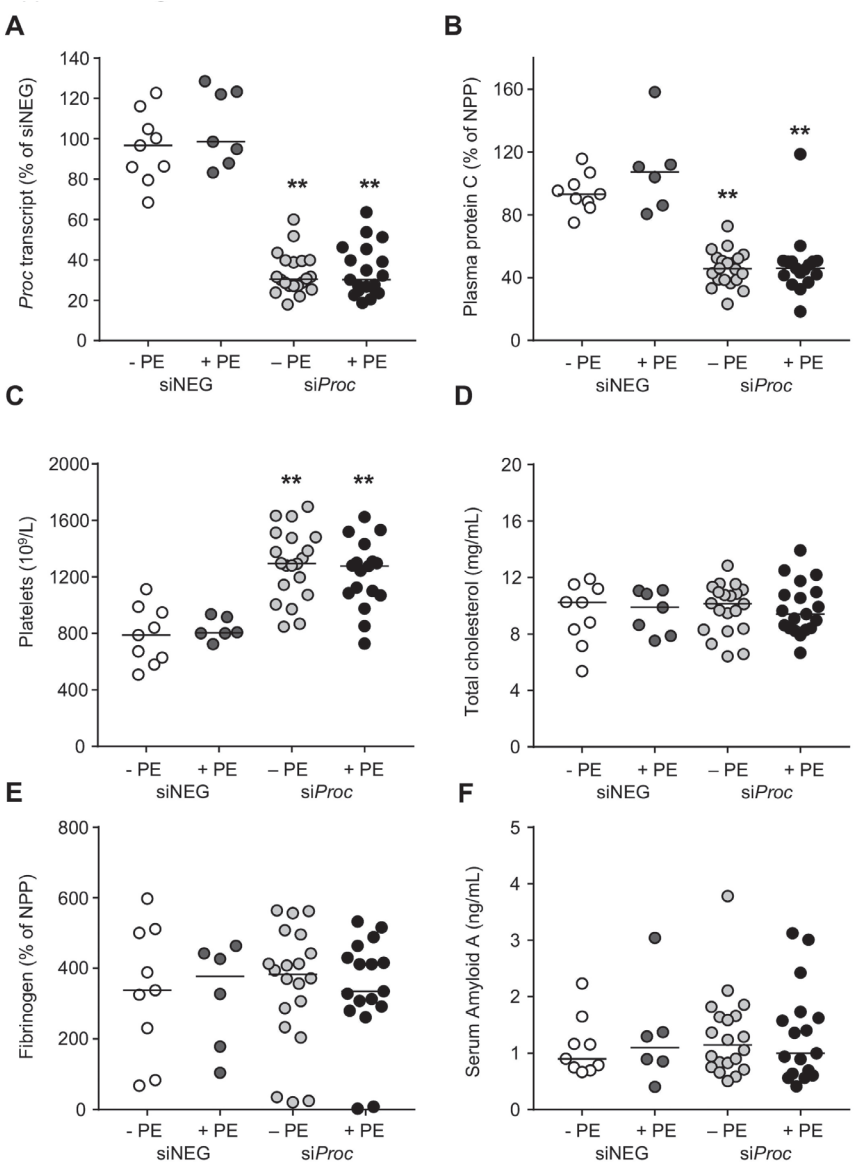


**Supplemental figure 7 | Liver, blood and plasma analysis of siNEG and si*Proc* treated *Apoe*$^{-/-}$ mice, with and without phenylephrine (PE).** (A) *Proc* transcript in the liver upon sacrifice (7 days after si*Proc* treatment), compared to the mean value of siNEG treated (100%), (B) Plasma protein C levels., compared to the mean value of siNEG treated (100%), (C) Whole blood platelet levels, (D) Plasma total cholesterol levels, (E) Plasma fibrinogen levels, measured by ELISA, and expressed as % of normal pool plasma. We did not have any reason to exclude outliers with a low value (e.g. due to coagulation upon blood withdrawal), (F) Serum Amyloid A levels. Black bars indicate the median. – PE: PBS control treated mice, + PE: Phenylephrine treated mice **: *P*<0.01 for siNEG vs. si*Proc*.





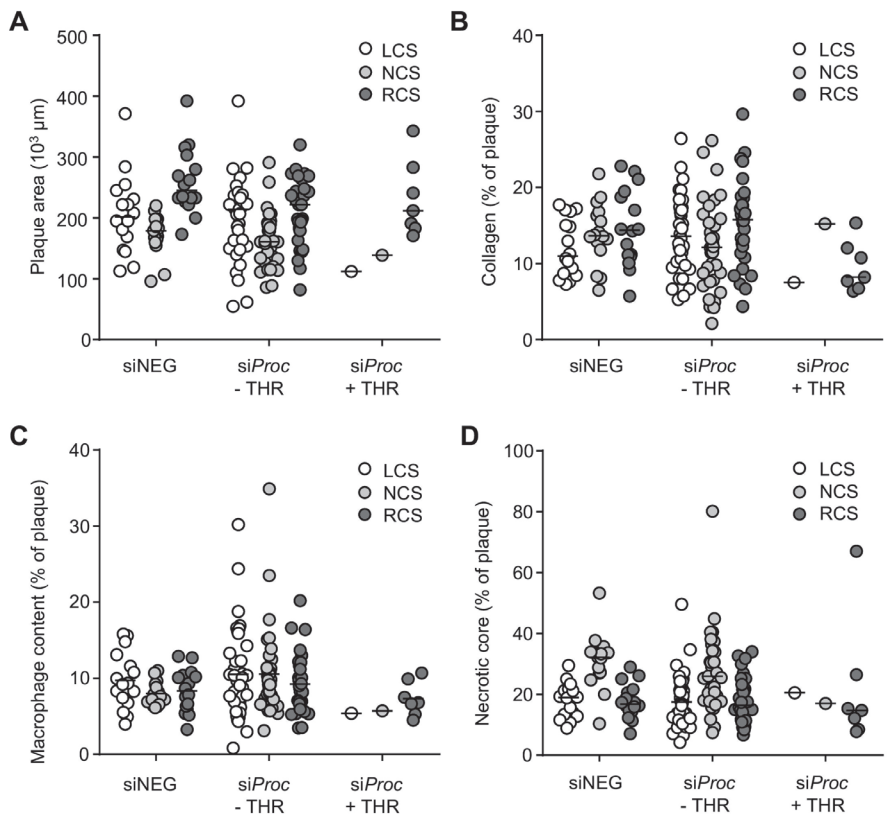


**Supplemental figure 8 | Composition of atherosclerotic plaques formed in the LCS, NCS, and RCS.** (A) Total plaque area, (B) Collagen, (C) Macrophage content, (D) Necrotic core. LCS: Left coronary sinus, NCS: Non-coronary sinus, RCS: Right-coronary sinus. For all panels, the indicated values represent an average measurement of three sections. Black bars indicate the median.